PROGRESS IN COLOR, COLORANTS AND COATINGS

available online @ www.pccc.icrc.ac.ir

Prog. Color Colorants Coat. 13 (2020), 131-141

Ministry of Science, Research and Technology
Institute for Color Science and Technology

Influence of Electrodeposition Method, Solvent and Nanoparticle Concentration on Polypyrrole Coatings for Corrosion Protection of Mild Steel

M. Zeidabadinejad, M. Shahidi Zandi*, M. M. Foroughi, H. Asadollahzadeh
Department of Chemistry, Kerman Branch, Islamic Azad University, P. O. Box: 7635131167, Kerman, Iran.

ARTICLE INFO

Article history:
Received: 24 May 2019
Final Revised: 22 Sept 2019
Accepted: 24 Sept 2019
Available online:23 Oct 2019

Keywords:
Electrosynthesized polypyrrole
Corrosion protection
Nanoparticles
Electrochemical impedance spectroscopy.

ABSTRACT

In this work, it was demonstrated that the anti-corrosion performance of the polypyrrole (PPy) coatings on mild steel can be affected by electrodeposition method, electrosynthesis solvent composition and ZnO nanoparticles concentration. Three different electrodeposition methods, namely, cyclic voltammetry, galvanostatic and potentiostatic techniques were empolyed. The anti-corrosion performance of the PPy coatings was investigated by electrochemical impedance spectroscopy. The PPy prepared by potentiostatic method exhibited the best performance against corrosion of mild steel in 3.5% NaCl solution. Then, different mixtures of H_2O/ethanol were investigated as electrosynthesis solvents for the preparation of PPy coatings on mild steel via optimized electrodeposition mode (i.e. potentiostatic). Evaluation of the prepared coatings introduced the pure water as the optimum solvent for the PPy electrodeposition. Lastly, the investigation of different concentrations of ZnO nanoparticles proved that the PPy coating containing 0.025% ZnO nanoparticles was the best coating against the corrosion of mild steel in the NaCl solution. Prog. Color Colorants Coat. 13 (2020), 131-141© Institute for Color Science and Technology.

1. Introduction

Conducting polymers have unique properties which make them suitable for many applications in both industrial and academic fields such as anti-corrosion coatings, sensors, supercapacitors and batteries [1-7]. Polypyrrole (PPy) as one of the most used conducting polymers has great advantages such as environmental and thermal stability, low cost and relatively easy polymerization [8-13].

A survey of literature indicates that little attention was paid to the optimum experimental conditions for preparing the optimum PPy coating for corrosion protection of mild steel including electrosynthesis method, solvent composition, and ZnO nanoparticle concentration.

The electropolymerization is generally achieved by potentiostatic (constant potential) or galvanostatic (constant current) methods [8]. These techniques are easier to describe quantitatively and have been therefore commonly utilized to investigate the nucleation mechanism and the macroscopic growth. Although potentiodynamic techniques such as cyclic voltammetry have been mainly used to examine the electrochemical behavior of the polymer film after electrodeposition, CV method was employed in this work for comparison.

The properties of PPy coatings for corrosion protection of alloy surface strongly depend on the

*Corresponding author: meshahidizandi@gmail.com
shahidi@iauk.ac.ir

synthesis parameters such as electrodeposition method, solvent composition and nano-size additives. Cyclic voltammetry (CV), galvanostatic (GS), and potentiostatic (PS) methods are some of the most important techniques for electrosynthesis of PPy coatings reported in the literature [8, 14]. The side reactions cannot occur at the alloy surface in the PS mode due to the application of a constant potential. The GS mode applies a constant current that is the preferred mode for preparing the PPy coatings on the large size electrodes [14]. The CV technique employs a triangular potential waveform to record the resulting current. However, the different modes of electrodeposition lead to manipulating the corrosion protection performance of PPy coatings.

As mentioned in the literature, CV-PPy and GS-PPy samples exhibit more organized microstructure together with typical layer by layer growth while PS-PPy shows relatively uniform 3D growth [14]. The composition of the solvent required for electrosynthesis of PPy coatings can affect the corrosion protection performance of the coatings. However, this field has been rarely reported in published papers [15, 16]. The performance of the coatings can be improved by doping the nanoparticles [17]. The concentration of the nanoparticles is a critical parameter influencing the corrosion protection of PPy coating [18].

The present work investigates the effects of various synthesis parameters including electrosynthesis method, solvent composition and nanoparticle concentration on the corrosion protection of PPy-coated mild steel. At first, the PPy films were deposited on the mild steel samples using CV, GS, and PS modes. Then, both the influence of different mixed solvent systems and various concentrations of ZnO nanoparticles have been investigated on the corrosion protection performance of the coatings. The corrosion protection performance of the resulting PPy samples was characterized after immersion in 3.5% NaCl solution by electrochemical impedance spectroscopy (EIS) and potentiodynamic polarization techniques.

2. Experimental

2.1. Materials

All chemicals and solvents were procured from Merck. Purification of pyrrole was performed by distillation under vacuum and then it was stored in the dark below 5 °C. Solutions were prepared by using distilled water.

2.2. Methods

2.2.1. Preparation of ZnO nanoparticles

ZnO nanoparticles were synthesized on the basis of the procedure which has been reported earlier [19]. The solutions of 0.45 M $Zn(NO_3)_2.4H_2O$ and 0.9 M NaOH were prepared in distilled water. Then, the sodium hydroxide solution was heated up to 55 °C. The heated NaOH solution under high-speed stirring was mixed with the zinc nitrate solution by drop-wise addition of the zinc nitrate solution (for about 40 min). After sealing the beaker at this condition for 2 h, the precipitates of ZnO nanoparticles were washed with both distilled water and ethanol and then dried in the air at about 60 °C. The final product was a white powder. X-ray diffraction (XRD) patterns were obtained by a Rigaku D-max C III, X-ray diffractometer using Ni-filtered Cu Kα radiation. Scanning electron microscopy (SEM) images were recorded by LEO-1455VP equipped with an energy dispersive X-ray spectroscopy.

Figure 1 shows the SEM images of ZnO nanoparticles. Figure 2 presents the XRD pattern of ZnO nanoparticles. All the peaks correspond to the reflections of ZnO nanoparticles (Peak List) which are in good accordance with the standard diffraction data of ZnO (JCPDS card no. 80-0075).

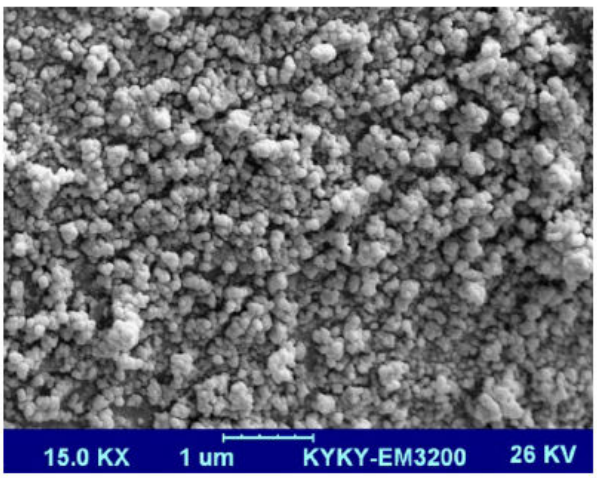

Figure 1: SEM images of ZnO nanoparticles.

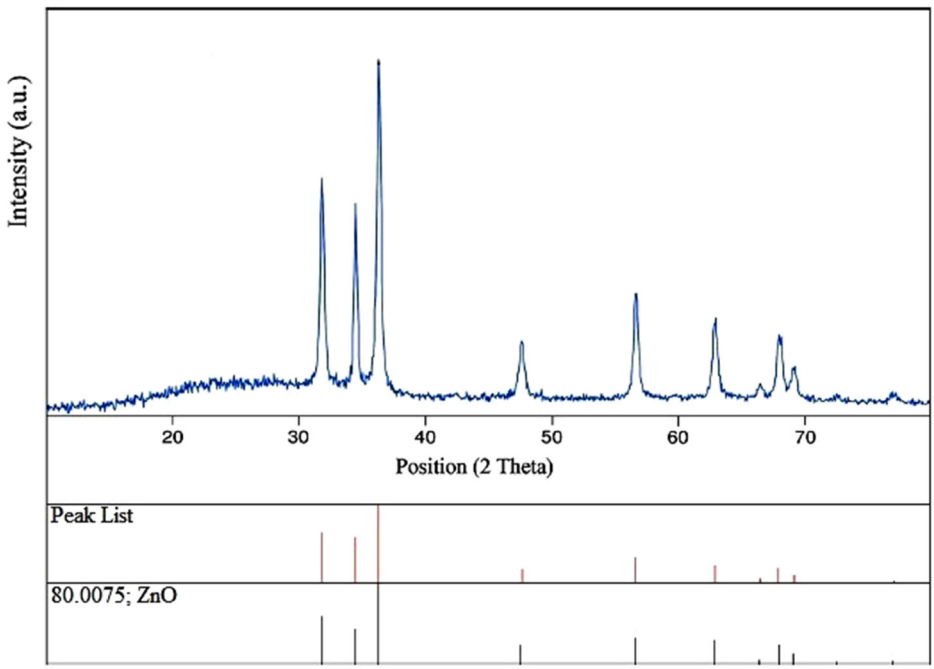

Figure 2: XRD pattern of ZnO nanoparticles.

2.2.2. Synthesis modes of PPy coated samples

The polypyrrole was synthesized by electropolymerization. Briefly, a solution obtained from mixing 0.1 M of pyrrole and 0.3 M oxalic acid in deionized water was used for the synthesis of polypyrrole. The electrosynthesis of PPy was performed by the following techniques: cyclic voltammetry method by potential scanning between +0.3 and +0.9 V at 100 mV/s for 20 cycles, galvanostatic technique at 5 mA/cm^2 for 5 min, and potentiostatic mode at 0.8 V for 3 min. A cell containing three electrodes was used for the electrosynthesis of PPy which consists of a disk of mild steel (100 mm^2) as working electrode, Ag/AgCl as the reference electrode, and a platinum rod as the counter electrode. Before the coating process, the mild steel surface was polished with abrasive papers (600-2500 grades) and washed with ethanol. After rinsing with distilled water, the PPy-coated mild steel electrodes were exposed to 3.5% NaCl solution.

The electropolymerization of PPy thin film is schematically illustrated in Figure 3. Briefly, in the first step, oxidation of pyrrole monomer forms pyrrole radicals at the electrode surface. With highest charge density at the α-position, the coupling between two radicals occurs, resulting in the formation of α,α′-dimers and the loss of two protons driving rearomatization. These aromatic dimers can further react with new radicals until the completion of the polymerization reaction. The aromatic dimer has an unpaired electron delocalized over two pyrrole rings which results in a lower oxidation potential compared to the monomer [8].

2.2.3. Synthesis media of PPy coated samples

Four volume ratios of water to ethanol were employed (1:3, 1:1, 3:1 and 1:0) for electrosynthesis of the PPy on the working electrodes. These PPy electrodes were denoted as PPy-1:3, PPy-1:1, PPy-3:1 and PPy-1:0 which were prepared from 1:3, 1:1, 3:1 and 1:0 volume ratios, respectively.

2.2.4. Effect of nanoparticle concentration

For preparation of coatings containing various concentrations of ZnO nanoparticles, different amounts of ZnO nanoparticle powder (0, 0.0125, 0.025, 0.05 and 0.1 g) was introduced to 100 mL solution of 0.1 M pyrrole and 0.3 M oxalic acid and then the electropolymerization of PPy was carried out by potentiostatic mode at 0.8 V for 3 min. Various PPy coatings containing 0, 0.0125, 0.025, 0.05 and 0.1 wt% of ZnO nanoparticles were prepared. The coating without ZnO nanoparticles (0%) was used as the blank.

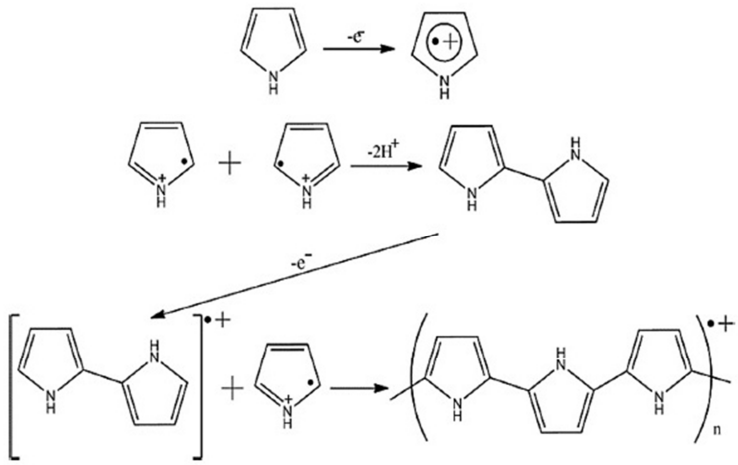

Figure 3: Mechanism of the pyrrole polymerization [8].

The current decreased with increasing the concentration of ZnO nanoparticles in the electrolyte solution. Therefore, addition of ZnO nanoparticles reduced the current of the monomer oxidation process at the same applied potentials. In addition, ZnO nanoparticles might act as a barrier and decrease direct interaction between pyrrole monomers and the surface of the mild steel.

2.2.5. Corrosion tests

For the EIS measurements, a sinusoidal potential signal of 10 mV amplitude at open circuit potential (OCP) was employed in the frequency range of 100 kHz-10 mHz. The EIS data were recorded by a potentiostat/galvanostat (Autolab Model PGSTAT-302N). A conventional three-electrode cell containing a Pt rod as the counter electrode, a saturated Ag/AgCl electrode as the reference electrode and the coated mild steel as the working electrode was used to measure the EIS data. The software of Nova 1.9 was employed for fitting the experimental EIS plots to the equivalent circuit.

Tafel plots were recorded for coated samples using a conventional three-electrode electrochemical cell with platinum rod as counter electrode and an Ag/AgCl as reference electrode. The working electrode was the coated mild steel sample. The NaCl (3.5%, w/w) solution was used as the corrosive environment.

3. Results and Discussion

3.1. Effect of electropolymerization mode

The deposition curves for electrosynthesis of PPy coatings on mild steel through potentiostatic, galvanostatic and cyclic voltammetry modes are shown in Figure 4. According to the shape of the deposition curves, it is possible to explain the mechanisms of the nucleation and growth. Figure 4a presents the electrodeposition plot of PPy coatings on mild steel obtained by the potentiostatic method at the constant potential of 0.8 V (vs Ag/AgCl). The initial increase in the current density is due to the formation of the double layer at the alloy/electrolyte interface. Afterward, the current decreases with decreasing the concentration of pyrrole due to the deposition of PPy on the mild steel electrode.

In the galvanostatic technique, a constant current is applied to the working electrode and the potential change is recorded. The electrodeposition plot of PPy coating at the constant current density of 5 mA/cm^2 is shown in Figure 4b. For oxidation of monomers to oligomers, not only a high potential is required at initial times, but also the constant potential should be high enough to complete the polymerization of the pyrrole [8, 14].

In the cyclic voltammetry, the resulting current during the application of potential sweep is recorded. The formation of PPy layer on the mild steel electrode through the oxidation of monomers into the radical cations corresponds to an increase in the current at +0.7 V (vs Ag/AgCl) (Figure 4c). As a characteristic feature of cyclic voltammetry, the break in the process of deposition between each cycle leads to a discontinuous growth, while the potential scan of the growing PPy layer produces uniform PPy microstructures [14, 20]. From the cyclic voltammetry data, it is possible to determine the optimum current density (5 mA/cm^2) and

electrodeposition potential (0.8 V vs Ag/AgCl) for PPy electrosynthesis through galvanostatic and potentiostatic methods, respectively.

EIS measurements are usually used to evaluate the corrosion protection performance of coated samples [21-23]. Figure 5 presents the impedance plots of different coated samples obtained after 4 h immersion in 3.5% NaCl solution.

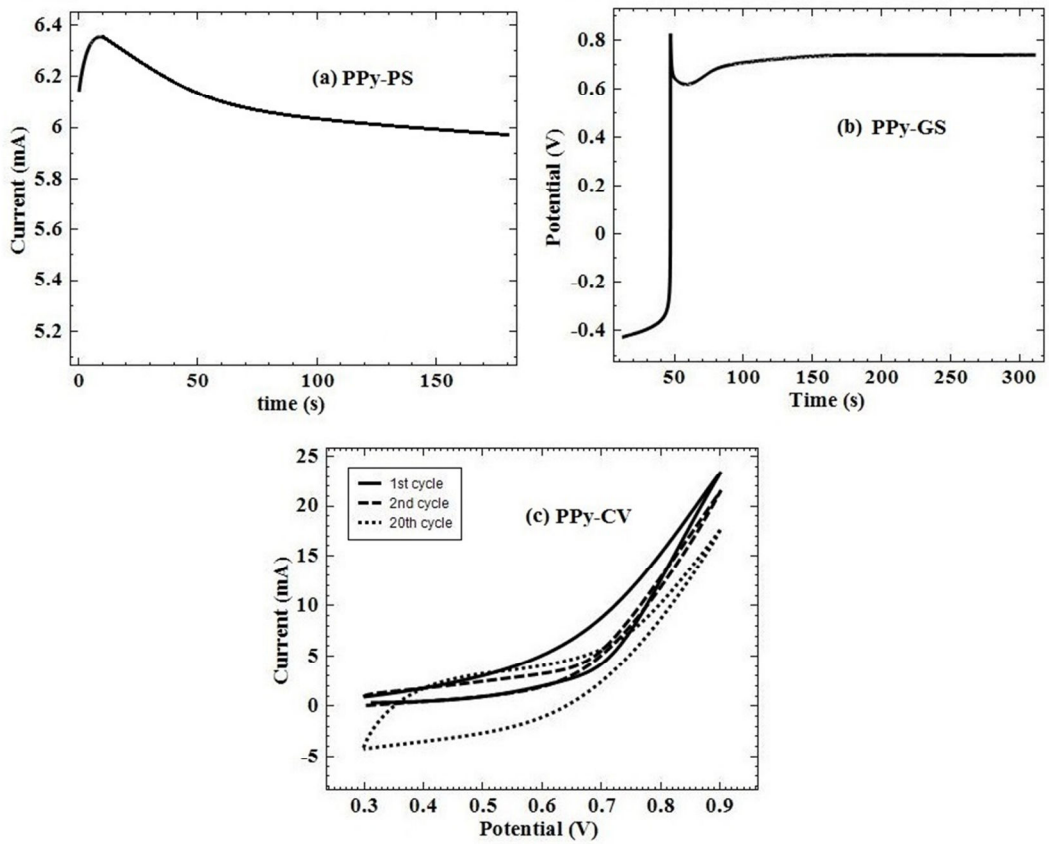

Figure 4: Electrosynthesis of polypyrrole coatings by different deposition methods: (a) potentiostatic, (b) galvanostatic and (c) cyclic voltammetry.

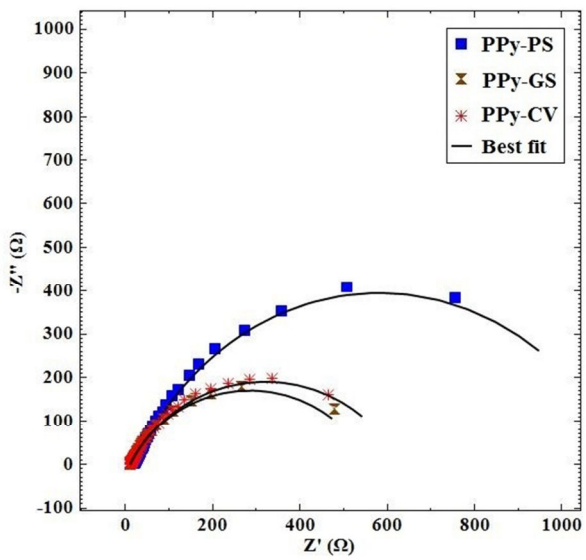

Figure 5: Nyquist plots of the PPy coatings obtained from different electrodeposition modes after 4 h of immersion in 3.5% NaCl solution.

In the literature, most of the EIS data arising from polymer coated samples exposed to corrosive media have been analyzed by the equivalent circuit shown in Figure 6 [24]. The equivalent circuit consists of solution resistance, Rs, charge transfer resistance, Rct, associated with the corrosion process on the alloy surface, pore resistance, Rpo, constant phase element (CPE) for the double layer, Qdl, and constant phase element for the coating, Qc. Because of the non-ideal capacitive behavior of the coatings, a constant phase element, Qdl, is used instead of pure capacitance. The impedance function of CPE is given by:

$$Z_{CPE} = 1/Y_0\,(j\omega)^n \quad (1)$$

where Y0 is the magnitude of CPE constant ($F.cm^{-2}.sn^{-1}$ or $sn.\Omega^{-1}.cm^{-2}$), ω is the angular frequency and n is the CPE exponent. When n=1, the CPE represents a pure capacitor and Y0 = C. Table 1 shows the fitted parameters for different coated samples. The highest value of pore resistance was obtained for PPy-PS which was higher than that of PPy-GS and PPy-CV samples (Figure 5). Therefore, the PPy-PS sample provided the highest corrosion protection of mild steel in NaCl solution.

Figure 7 shows the Tafel polarization curves of different coated samples obtained after 4 h immersion in 3.5% NaCl solution. The relevant parameters are listed in Table 2. The value of corrosion current for PPy-PS coating was lower than that of other samples. Therefore, the PPy coating was the best protective PPy coating on mild steel surface.

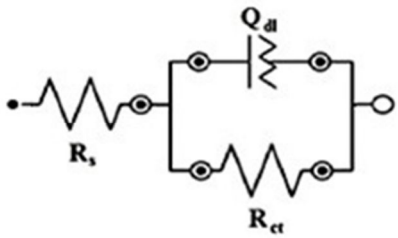

Figure 6: Equivalent circuit.

Table 1: Impedance parameters for PPy coating samples prepared by different modes of electrodeposition on mild steel after 4 h of immersion in 3.5% M NaCl solution.

Sample	$R_{po}/\Omega.cm^2$	$Y_0/\mu mho$	n
PPy-PS	1125	589	0.707
PPy-GS	550	735	0.711
PPy-CV	630	595	0.704

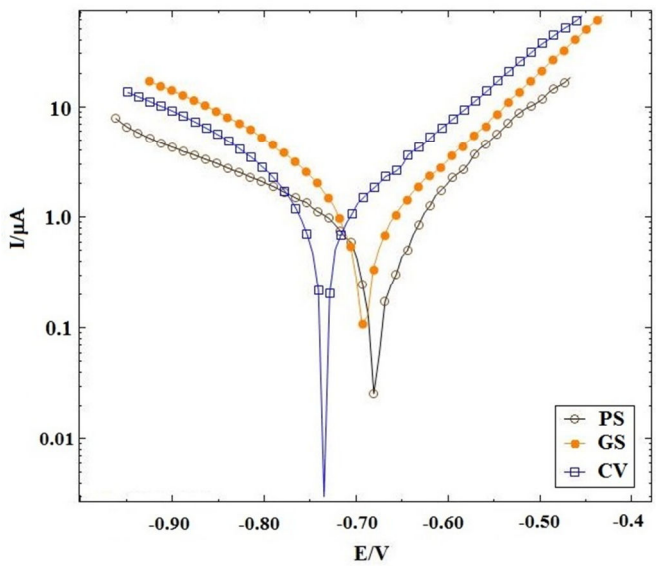

Figure 7: Tafel plots of the PPy coatings obtained from different electrodeposition modes after 4 h of immersion in 3.5% NaCl solution.

Table 2: Tafel parameters for PPy coating samples prepared by different modes of electrodeposition on mild steel after 4 h of immersion in 3.5% M NaCl solution.

Sample	i_{corr}/μA	E_{corr}/mV
PPy-CV	1.1	-735
PPy-GS	1.0	-695
PPy-PS	0.88	-680

3.2. Effect of synthesis solvent

In order to improve the corrosion protective behavior of the PPy coatings, various binary mixtures were employed as the solvent for electrosynthesis of PPy films. The electrochemical impedance spectroscopy was utilized to investigate the corrosion protective behavior of the PPy coatings prepared using different binary mixtures. The impedance plots of different PPy coated samples after immersion in 3.5% NaCl solution are shown in Figure 8. The equivalent circuit represented in Figure 6 was used to fit the impedance plots of the PPy coated samples. The circuit parameters are listed in Table 3.

Figure 9 shows the plot of Rpo vs. H_2O% of the solvents employed for the PPy electrosynthesis. The larger pore resistance (Rpo) value for the PPy-1:0 coating compared to those of other PPy coated samples imply that the water is the suitable solvent for preparing the best protective PPy coating by the potentiostatic electrosynthesis.

Figure 10 shows the Tafel plots of different PPy coatings after immersion in 3.5% NaCl solution. Tafel parameters are listed in Table 4. Therefore, the lower corrosion current value for the PPy-1:0 coating compared to those of other PPy coated samples imply that the water is the suitable solvent for preparing the best protective PPy coating.

Table 3: Impedance parameters for PPy coating samples prepared in different water to ethanol ratios on mild steel after 4 h of immersion in 3.5% M NaCl solution.

Sample	R_{po}/Ω.cm^{-2}	Y_0/μmho	n
PPy-1:3	66	2125	0.817
PPy-1:1	103	1245	0.813
PPy-3:1	434	75	0.689
PPy-1:0	1125	589	0.707

Table 4: Impedance parameters for PPy coating samples prepared by different concentrations of ZnO nanoparticles after 4 h of immersion in 3.5% M NaCl solution.

Sample	R_{po}/Ω.cm^2	R_{ct}/Ω.cm^2
Blank	1125	-
0.0125%	1650	-
0.025%	2270	-
0.05%	121	895
0.1%	73	642

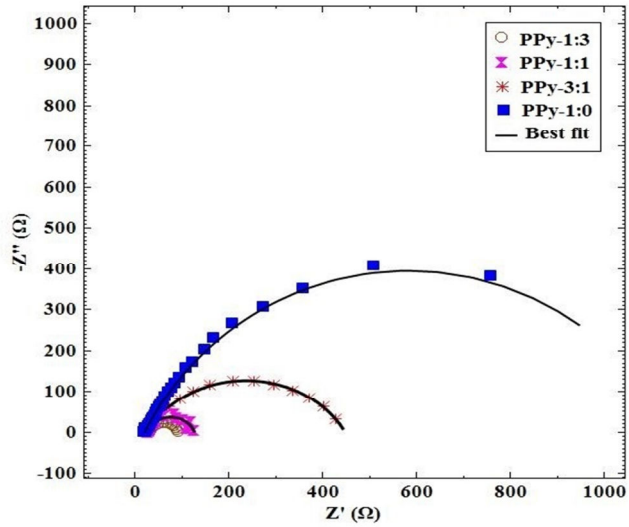

Figure 8: Nyquist plots of the PPy coatings prepared from different solvent compositions after 4 h of immersion in 3.5% NaCl solution.

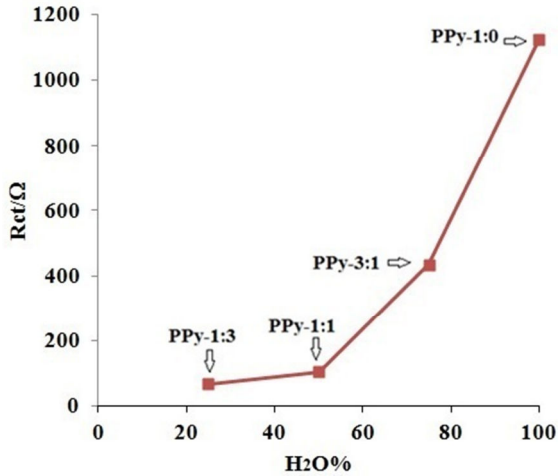

Figure 9: The plot of R_{po} against solvent conposition employed for the PPy electrosynthesis.

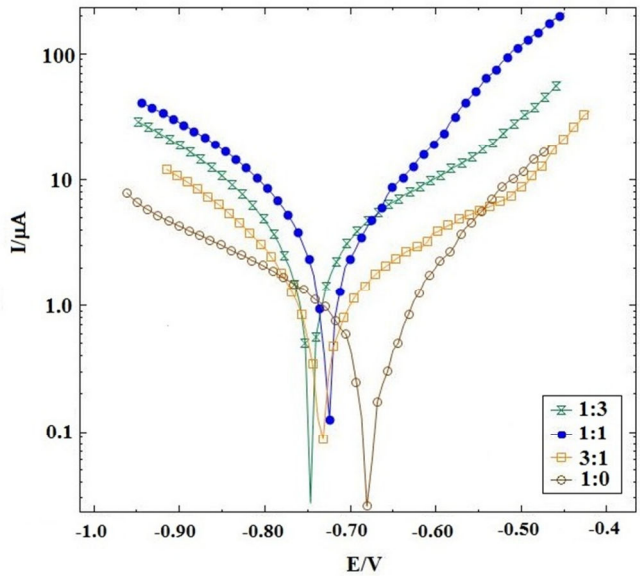

Figure 10: Tafel plots of the PPy coatings prepared from different solvent compositions after 4 h of immersion in 3.5% NaCl solution.

3.3. Effect of nanoparticle concentration

Figure 11 shows the electrochemical impedance spectra of the PPy coatings without and with various concentrations of ZnO nanoparticles after 4 h immersion in 3.5% NaCl solution. The Nyquist plots of the PPy coated samples containing 0.1% and 0.05% ZnO nanoparticles showed two semicircles (Figure 11). These Nyquist plots were fitted to the equivalent circuit given in Figure 6. This pattern, typical for two Randles circuits connected in parallel, confirmed the presence of two different phases in the coating containing nanoparticles as filler. High-frequency semicircle at the left-hand side of a curvature is usually related to the PPy phase of the coating regardless of the amount of nanoparticle filler with pore resistance within the range from 73 to 121Ω. Low-frequency semicircle on the right-hand side of a curvature corresponds to the metal response during the corrosion process [25]. This phase changed its charge transfer resistance from 895 to 642Ω when ZnO nanoparticle content increased from 0.05 to 0.1%.

On the other hand, the Nyquist plots of the coated samples containing 0.025 and 0.0125% ZnO nanoparticles showed only one relaxation time [26]. This semicircle is related to the protective properties of the PPy coatings.

Table 5 lists the impedance parameters for different PPy coated samples. Figure 12 presents the Rpo vs. ZnO% plot of the coated samples. The Rpo value of 0.025% coated sample was higher than those of other coated samples after 4 h immersion. Figure 12 clearly shows that the pore resistance increased with the increase of nanoparticle concentration in the range of 0–0.025% and then it decreased with increasing nanoparticle concentration up to 0.1%. In general, the surface roughness of the coating increases and the aesthetic properties of the coating decrease with increasing the nanoparticle percent in the coated samples. It can be concluded from Figure 12 that the optimum coating is the coating containing 0.025% ZnO nanoparticle.

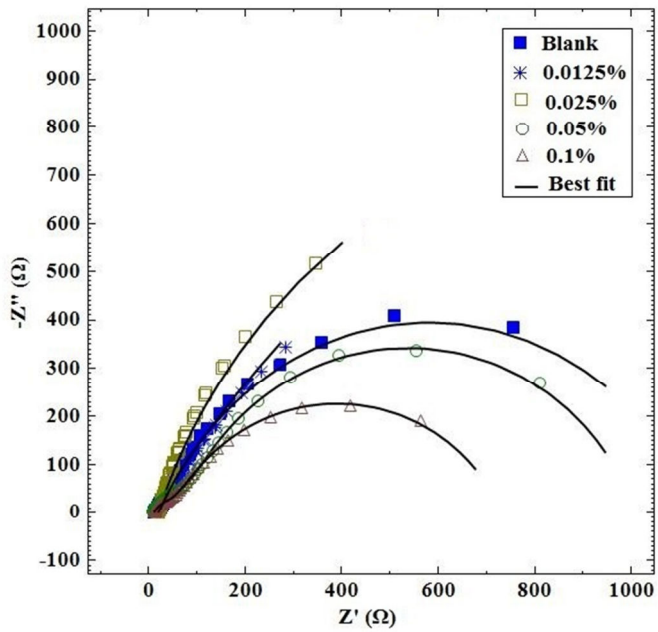

Figure 11: Nyquist plots of the PPy coatings without (blank) and with different concentrations of ZnO nanoparticles recorded at 4 h after immersion in 3.5% NaCl solution.

Table 5: Impedance parameters for PPy coating samples prepared by different concentrations of ZnO nanoparticles after 4 h of immersion in 3.5% M NaCl solution.

Sample	$R_{po}/\Omega.cm^2$	$R_{ct}/\Omega.cm^2$
Blank	1125	-
0.0125%	1650	-
0.025%	2270	-
0.05%	121	895
0.1%	73	642

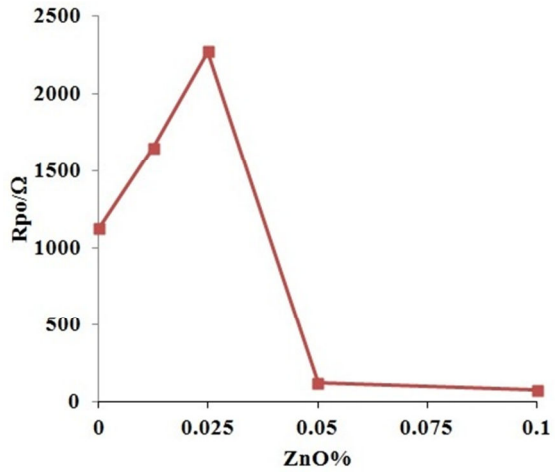

Figure 12: The plots of R_{po} vs ZnO% for different PPy coating samples after 4 h of immersion in 3.5% NaCl solution.

4. Conclusions

Three different electrodeposition methods were employed for polypyrrole (PPy) coating synthesis including cyclic voltammetry, galvanostatic and potentiostatic modes in order to prepare the optimum PPy coating for corrosion protection of mild steel in 3.5% NaCl solution. The electrochemical properties of PPy coatings were investigated by electrochemical impedance spectroscopy (EIS). Among three different PPy electrosynthesized samples, the PPy electrosynthesized by the PS mode provided the optimum protection of mild steel against corrosion. In addition, different binary mixtures of H_2O/ethanol were investigated as electrosynthesis solvents for the preparation of PPy coatings on mild steel by the potentiostatic mode. The results showed that the pure water was the optimum solvent for the PPy electrodeposition. Lastly, the investigation of ZnO nanoparticles concentration showed that the synthesis solution containing 0.025% ZnO nanoparticle can lead to the production of the best coating against corrosion of mild steel in NaCl solution.

Acknowledgments

The authors would like to express their deep gratitude to the Iranian Nano Council for supporting this work.

5. References

1. M. Hosseini. L. Fotouhi. A. Ehsani, M. Naseri, Enhancement of corrosion resistance of polypyrrole using metal oxide nanoparticles: Potentiodynamic and electrochemical impedance spectroscopy study, *J. Colloid Interface Sci.,* 505(2017), 213-219.
2. Y. Lei. N. Sheng. A. Hyono. M. Ueda, T. Ohtsuka, Influence of pH on the synthesis and properties of polypyrrole on copper from phytic acid solution for corrosion protection, *Prog. Org. Coat.,* 77(2014), 774-784.
3. S. Lee, H. Lee, Electrodeposition of Conducting Polymers on Copper in Nonaqueous Media by Corrosion Inhibition, *J. Electrochem. Sci. Technol.,* 3(2012), 85-89.

4. V. Venugopal. V. Venkatesh. R. G. Northcutt. J. Maddox, V. B. Sundaresan, Nanoscale polypyrrole sensors for near-field electrochemical measurements, *Sens. Actuators, B,* 242(2017), 1193-1200.
5. A. Bahloul. B. Nessark. E. Briot. H. Groult. A. Mauger. K. Zaghib, C. M. Julien, Polypyrrole-covered MnO_2 as electrode material for supercapacitor, *J. Power Sources,* 240(2013), 267-272.
6. D. P. Dubal. S. H. Lee. J. G. Kim. W. B. Kim, C. D. Lokhande, Porous polypyrrole clusters prepared by electropolymerization for a high performance supercapacitor, *J. Mater. Chem.,* 22(2012), 3044-3052.
7. J. S. Shayeh. S. O. R. Siadat. M. Sadeghnia. K. Niknam. M. Rezaei, N. Aghamohammadi, Advanced studies of coupled conductive polymer/metal oxide nano wire composite as an efficient supercapacitor by common and fast fourier electrochemical methods, *J. Mol. Liq.,* 220(2016), 489-494.
8. S. Sadki. P. Schottland. N. Brodie, G. Sabouraud, The mechanisms of pyrrole electropolymerization, *Chem. Soc. Rev.,* 29(2000), 283-293.
9. C. Shi, I. Zhitomirsky, Electrodeposition of 0composite polypyrrole–carbon nanotube films, *Surf. Eng.,* 27(2011), 655-661.
10. K. Qi. Y. Qiu. Z. Chen, X. Guo, Corrosion of conductive polypyrrole: Galvanic interactions between polypyrrole and metal substrates, *Corros. Sci.,* 91(2015), 272-280.
11. A. El Jaouhari. M. Laabd. E. A. Bazzaoui. A. Albourine. J. I. Martins. R. Wang. G. Nagy, M. Bazzaoui, Electrochemical and spectroscopical studies of polypyrrole synthesized on carbon steel from aqueous medium, *Synth. Met.,* 209(2015), 11-18.
12. H. Arabzadeh. M. Shahidi, M. M. Foroughi, Electrodeposited polypyrrole coatings on mild steel: Modeling the EIS data with a new equivalent circuit and the influence of scan rate and cycle number on the corrosion protection, *J. Electroanal. Chem.,* 807(2017), 162-173.
13. H. Arabzadeh. M. Shahidi Zandi, M. M. Foroughi, Interpretation of Electrochemical Noise Signals Arising from Symmetrical and Asymmetrical Electrodes Made of Polypyrrole Coated Mild Steel, *Prog. Color Colorants Coat.,* 12(2019), 25-32.
14. F. Wolfart. D. P. Dubal. M. Vidotti. R. Holze, P. Gómez-Romero, Electrochemical supercapacitive properties of polypyrrole thin films: influence of the electropolymerization methods, *J. Solid State Electrochem.,* 20(2016), 901-910.
15. N. Aravindan, M. V. Sangaranarayanan, Influence of solvent composition on the anti-corrosion performance of copper–polypyrrole (Cu–PPy) coated 304 stainless steel, *Prog. Org. Coat.,* 95(2016), 38-45.
16. R. L. Zhu. G. X. Li. J. H. Zheng. J. W. Jiang, H. B. Zeng, Influence of electrosynthesis potential on corrosion performance of polypyrrole coated stainless steel and its mechanism research, *Surf. Eng.,* 25(2009), 156-162.
17. G. S. Sajadi. S. M. A. Hosseini. M. J. Bahrami, M. Shahidi, Electrochemical evaluation of polyvinyl butyral coating containing polypyrrole/ZnO nanocomposite for corrosion protection of Al Alloy, *Prog. Color Colorants Coat.,* 10(2017), 205-216.
18. A. M. Kumar, N. Rajendran, Electrochemical aspects and in vitro biocompatibility of polypyrrole/TiO_2 ceramic nanocomposite coatings on 316L SS for orthopedic implants, *Ceram. Int.,* 39(2013), 5639-5650.
19. A. B. Moghaddam. T. Nazari. J. Badraghi, M. Kazemzad, Synthesis of ZnO nanoparticles and electrodeposition of polypyrrole/ZnO nanocomposite film, *Int. J. Electrochem. Sci.,* 4(2009), 247-257.
20. S. Sadki. P. Schottland. N. Brodie, G. Sabouraud, The mechanisms of pyrrole electropolymerization, *Chem. Soc. Rev.,* 29(2000), 283-293.
21. Y. H. Kim. Y. S. Kwon. M. Y. Shon, M. J. Moon, Corrosion protection performance of PVDF/PMMA-blended coatings by electrochemical impedance method, *J. Electrochem. Sci. Technol.,* 9(2018), 1-8.
22. M. C. S. S. Macedo. I. C. P. Margarit-Mattos. F. L. Fragata. J. B. Jorcin. N. Pébère, O. R. Mattos, Contribution to a better understanding of different behaviour patterns observed with organic coatings evaluated by electrochemical impedance spectroscopy, *Corros. Sci.,* 51(2009), 1322-1327.
23. M. Sababi. J. Pan. P. E. Augustsson. P. E. Sundell, P. M. Claesson, Influence of polyaniline and ceria nanoparticle additives on corrosion protection of a UV-cure coating on carbon steel, *Corros. Sci.,* 84(2014), 189-197.
24. F. Mansfeld, Use of electrochemical impedance spectroscopy for the study of corrosion protection by polymer coatings, *J. Appl. Electrochem.,* 25(1995), 187-202.
25. J. M. Sanchez-Amaya. R. M. Osuna. M. Bethencourt, F. J. Botana, Monitoring the degradation of a high solids epoxy coating by means of EIS and EN, *Prog. Org. Coat.,* 60(2007), 248-254.
26. D. E. Tallman. K. L. Levine. C. Siripirom. V. G. Gelling. G. P. Bierwagen, S. G. Croll, Nanocomposite of polypyrrole and alumina nanoparticles as a coating filler for the corrosion protection of aluminium alloy 2024-T3, *Appl. Surf. Sci.,* 254(2008), 5452-5459.

How to cite this article:

M. Zeidabadi, M. Shahidi Zandi, M. M. Foroughi, H. Asadollahzadeh, Influence of Electrodeposition Method, Solvent and Nanoparticle Concentration on Polypyrrole Coatings for Corrosion Protection of Mild Steel. Prog. Color Colorants Coat., 13 (2020), 131-141.